2021

Petrology of an oxidized blueschist cobble from the San Onofre Breccia, California, USA

Alaina A. Helm
Oberlin College

PETROLOGY OF AN OXIDIZED BLUESCHIST COBBLE FROM THE SAN ONOFRE BRECCIA, CALIFORNIA, USA

By Alaina Helm

Advisor: Dr. F. Zeb Page

Honors Thesis

Oberlin College Geology Department

April 2021

Abstract

The mid-Miocene San Onofre Breccia (SOB) found along the southern California borderlands contains clasts of several lithologies including high-pressure metamorphic rocks commonly thought to be shed from the Catalina Schist. Sorensen concluded the San Onofre Schist was part of the Franciscan Complex, although at that time the Catalina subduction was considered to be part of the Franciscan Complex. In this study, a ~10 cm cobble collected from the San Onofre type locality was studied to describe its mineralogy and estimate its conditions of metamorphism. The cobble is composed of glaucophane (35%) + epidote (15%) + garnet (13%) + phengite (12%) + omphacite (7%), with minor quartz, sphene, apatite, chlorite, rutile, and zircon components. Garnets (~3 mm) are zoned with $Alm_{56}Grs_{27}Pyp_{3}Sps_{14}$ cores and $Alm_{66}Grs_{25}Pyp_{9}$ rims. Blue amphibole in the rock is intermediate between glaucophane and barroisite. Garnet and epidote porphyroblasts occur within a blue amphibole (intermediate between glaucophane and barroisite) matrix with minor pyroxene. Prismatic epidote is aligned with the dominant foliation. Phengite is present as smaller crystals throughout the matrix and surrounding the garnets. Dark green clinopyroxene $Ac_{13}Jd_{34}Di_{39}Hd_{11}CaTs_{1}$ is notably rich in Fe^{3+}. I estimated metamorphic conditions using Equilibrium Assemblage Modeling in the MnNCKFMASHTO system. T-X and P-X diagrams were used to estimate the amount of additional O_2 in the system. Results suggest metamorphism at 520°C and 16kbar with the addition of around 0.3 wt% $O_2$to reproduce the observed Fe^{3+}-rich assemblages. Under these conditions, calculated modes for major minerals match those observed in the sample. A potential source of error includes uncertainty in Fe^{3+}-bearing solution models, which predict more Fe^{3+} in Amp than in Cpx, the opposite

of what is observed. This rock more closely resembles Franciscan garnet blueschist tectonic blocks from Northern California and Catalina in mineralogy and pressure-temperature (P-T) conditions than younger, lower-grade blueschists from Catalina. Geochronology will further help place this sample in multiple episodes of Californian subduction cycles.

Introduction

In this study, the tectonic origins of blueschist from the San Onofre Breccia is examined through petrographic analysis. Mineralogical, geochemical, and thermobarometry techniques are used to constrain how the blueschist fits into the subduction cycles evident in southern California, and provide a well constrained context for their metamorphic origin. The sample, 18So1, used in this analysis was collected at San Onofre proper. The sample is a garnet-epidote blueschist that contains a garnet vein. It is from a canyon that is forming behind a scarp in the beachfront, in a region well known for blueschists that are weathered out of the San Onofre Breccia. The coordinates of the location are 22.236996°, -117.536766°. This project compares 18So1 to similar blueschists found in the literature known to originate from both the Catalina and Franciscan subduction zones to better understand the San Onofre Blueschist's tectonic origin.

The San Onofre Breccia is a Miocene-aged sedimentary deposit located between Los Angeles and San Diego, California (Fig. 1). The San Onofre Breccia was first examined nearly a century ago as California geologist A.O. Woodford first sought to

understand the regional patterns and distinct lithology (Woodford 1924, 1925). The formation consists of “cobble conglomeratic, coarse- to very coarse-grained sandstone” (Stuart, 1974). The clasts contain a variety of metamorphic rock types including schists and granitic material. The metamorphic cobbles within the sedimentary sequence are often thought to derive from the Catalina Schist (Fig. 1) as paleocurrents indicate they accumulated from the west in a “fan-shaped gravel wedge” (Stuart, 1974). The abundance of blueschist and glaucophanic greenschist within the sedimentary formation is theorized to come “almost entirely from a Catalina Schist terrane” (Vedder and Howell, 1976). As shown in Figure 1, the Catalina Schist is located off the coast of California at Santa Catalina Island as well as in submarine outcrops. These units could have been transported to be deposited in the San Onofre Breccia by east moving paleocurrents. Paleocurrent indicators do seem to contradict Yeats et al. (1970), who describe a northeastern paleo current forming the San Onofre Breccia on the Santa Cruz Islands, whereas Stuart et al. (1974) describes the San Onofre Breccia in the Tijuana Area being formed by a paleocurrent coming from the west. The San Onofre lithology is likely submarine in origin.

Yeats et al. (1970) argued that the Catalina Schist was exhumed when a “granitic structural block” broke apart from the Santa Monica Mountains in the Miocene leaving behind a Catalina Schist facies basement. The early to mid Cretaceous Catalina Schist is exposed on Catalina Island and on the Palos Verdes Peninsula in the Los Angeles region and represents part of an accretionary complex (e.g., Platt et al. 2020). Platt (1975) described subduction material on Catalina Island consisting of blueschist, greenschist, and amphibolite units that were metamorphosed at high pressures and

temperatures before some retrograde metamorphosis occurred and the units underwent “postmetamorphic thrusting”. These materials are argued to be part of a Catalina subduction zone, instead of part of the Franciscan as they had been previously attributed to (Platt et al. 1975). Study of the Catalina Schist Terrane indicates that the San Onofre Breccia’s formation is roughly synchronous with the exhumation of the Catalina Schist Terrane in the early- middle Miocene (Wright, 1991; Crouch and Suppe, 1993). Tectonic models use cooling histories to indicate that by the end of the Cretaceous, the terrane had been exhumed to within ~10 km of the Earth’s surface (Grove et al. 2008).

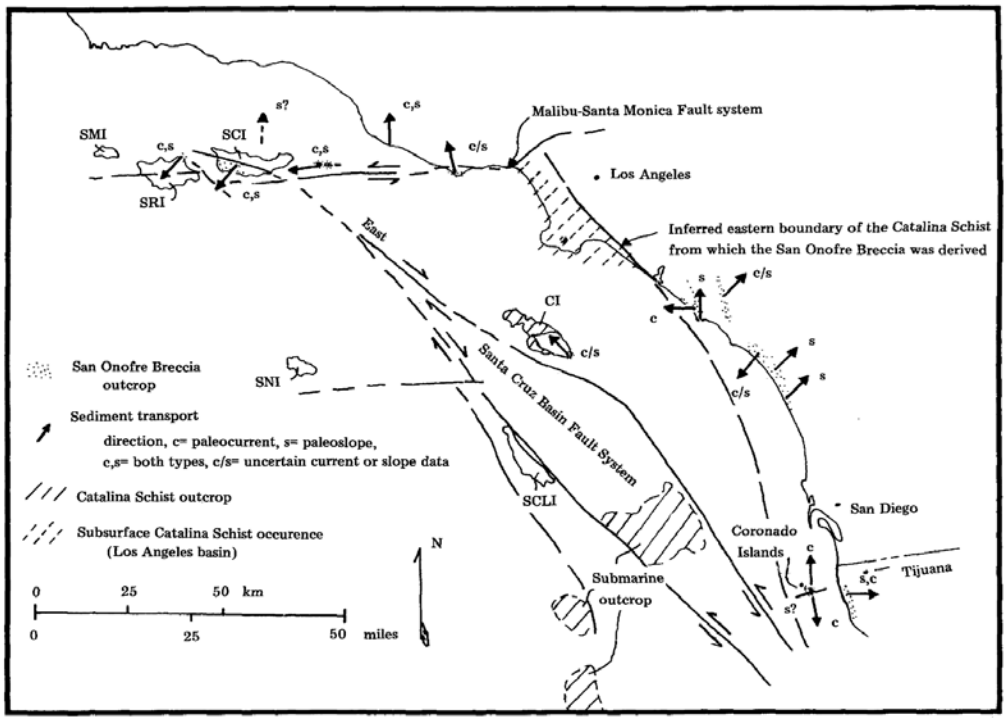

Figure 1. Map from Stuart et al. (1974) showing the locations of the San Onofre Breccia with transport directions and fault systems.

The only prior petrological analysis of clasts from the San Onofre Breccia were completed by Sorensen (1978) when the Catalina Schist was considered to be equivalent to the Franciscan Complex. It has since been determined that the Catalina Schist Terrane is an early-middle Cretaceous subduction complex created “during nascent subduction at ca. 115 Ma” (Grove et al. 2008) while the Franciscan Complex is of late Jurassic age dated between 138 to 159 Ma (Wakabayashi 1999), and is found from Northern to Baja California. The Catalina Schist was considered to be Franciscan until 1986, when it was determined that younger ages and lower pressure-temperature estimates differentiated the Catalina Schist from the Franciscan. While not currently prevalent within the Los Angeles. and San Diego region, Grove et al. (2008) suggests that Franciscan material existed offshore and was included in the Catalina mélange, describing franciscan exposures as far south as Baja California, giving the Franciscan a range of over 600 miles. Grove proposes that an Upper Cretaceous forearc complex is represented at the “margin of the Peninsular Ranges batholith” which provides a potential alternative source for Franciscan as opposed to Catalina Schist material for the San Onofre Breccia (Grove et al. 2008). This batholith, which lies alongside the San Onofre Breccia to the Northeast, is proposed to be chemically related to the Catalina schist.

Metamorphic clasts within the San Onofre Breccia support the hypothesis that the Catalina Schist “Terrane underlies much of what is known as the Inner Borderland, extending from Santa Cruz Island in the north at least as far south as San Diego“ (Platt et al. 2020). Additionally, the classification of San Onofre sediments as part of the Catalina Schist Terrane is used to support the hypothesis that exposures of Catalina

Schist on Catalina Island are broadly representative of the entire schist terrane (Stuart 1979, Grove et al. 2008).

Methods

A petrographic analysis was performed using optical microscopy and the Tescan Vega 3 Scanning Electron Microscope and Oxford Instruments XMaxN80 detector Energy Dispersive X-Ray Spectrometer (SEM-EDS) with AZtec software at Oberlin College. I derived compositional data of individual minerals using point spectra and built-in virtual standards while bulk composition was calculated with compositional mapping using SEM-EDS and Back Scattered Electron (BSE) imaging. Compositional mapping was completed by using the automation feature in the AZtec nanoanalysis program on the EDS. The computer was set to take a series of images following a grid pattern to collect BSE and EDS images over an entire thin section sample. AZtec was then used to identify the modes of minerals for the complete section. The bulk composition was calculated by multiplying the modes by the average composition of each phase. Mineral compositions were calculated using wt% oxides and cation normalizations. All iron was quantified as FeO, but Fe^{3+} was estimated using charge balance. Formulae of amphiboles were calculated according to end member proportions using an excel spreadsheet and sight assignment approaches recommended by Locock (2014) following IMA 2012 recommendations for naming (Hawthorne et al. 2012).

Equilibrium assemblage diagrams (EADs) were created using the free-energy minimization program Perple_X (Connolly 1990, 2005) which uses Holland and Powell's Thermocalc database updated in 2011 (version 6.2). Such analyses create a phase

diagram specific to the rocks' bulk composition, which will allow for further comparison between the Franciscan and Catalina terrane through pressure-temperature estimates. Equilibrium assemblage modeling diagrams, also called psuedosections are created using phase equilibria and thermodynamic properties assuming chemical equilibrium to ascertain the stability of a mineral assemblage over a range of pressure-temperature conditions. Equilibrium Assemblage Models were run using the system MnNCKFMASHTO. This chemical system was selected because titanium allows for rutile stability, manganese is critical for the stability of garnet, and oxygen allows for the consideration of Fe^{3+}. The solution models used were epidote (Holland and Powell 2011), garnet (White et al. 2014), omphacite (Green et al. 2007), chlorite (White et al. 2014), phengite (Holland and Powell 2003), feldspar (Fuhrman and Lindsley 1998), Ilmenite (White et al. 2014) and clinoamphibole (Diener et al. 2007). Ferric iron present in the assemblage could not be predicted by the solution models without the addition of extra oxygen to the system. The amount of oxygen added to the model was determined by using a series of T-X diagrams that were created using Perple_X. This method uses a fixed pressure to show how changes in composition alter which mineral assemblages are stable in a range of temperature conditions. Using this technique, we modelled fO_2 by adding additional O_2 to the model which allowed us to reproduce the observed assemblage. Exact calculation of fO_2 has not yet been completed, but is a logical next step. All models were calculated with excess H_2O. Pressure temperature estimates were made with isomodes calculated using the WERAMI tool in Perple_X and plotted with PYWERAMI. Isomode plots create a series of lines similar to a topographic map detailing the amount (or mode) of each mineral stable at any given point. Plotting modes

of solution models with PYWERAMI on equilibrium assemblage diagrams calculated using Perple_X allowed for the analysis of pressure-temperature points where the amounts of epidote, amphibole, and garnet coincide with mineral modes observed in the sample.

Results

Petrography and Geochemical Data

Figure 2. 18So1 hand sample. Note the garnet vein.

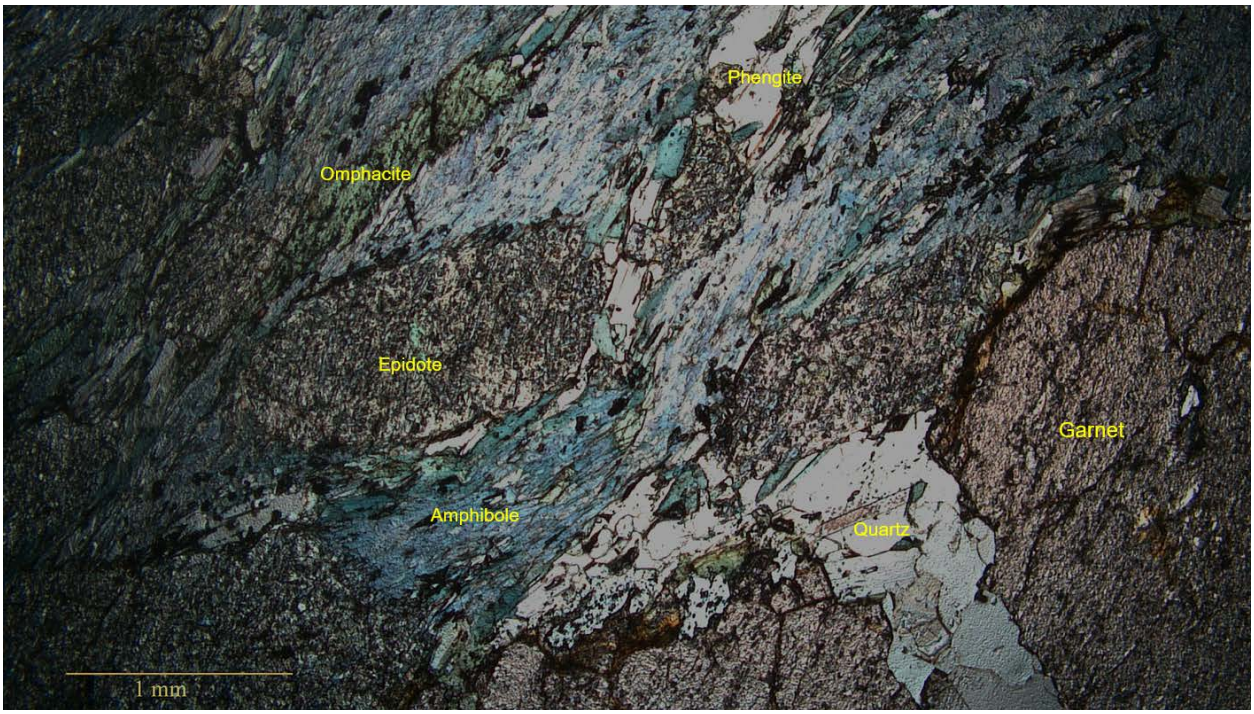

Figure 3. A photo of a thin section of the sample under plain polarized light.

The sample used in this analysis (18SO1) is a garnet-epidote blueschist (Fig. 2). The shist's assemblage is Amph (35%) + Ep (15%) + Grt (13%) + Ph (12%) + CPX (7%) with minor quartz, sphene, apatite, chlorite, rutile, and zircon. Major element bulk composition calculated from SEM-EDS mineral analysis and mode calculation is reported in Table 1.

The sample is primarily composed of blue amphibole. In thin section, the amphibole is relatively patchy in color, appearing colorless, purple, pink, blue and is pleochroic (Fig. 3). The amphibole forms the matrix of the sample with frequent garnet and epidote porphyroblasts and a few rare pyroxene crystals within the matrix. Amphibole composition falls within the sodium and sodium-calcium amphibole subgroup bordering in composition between glaucophane, barrosite, katophorite, and winchite when classified using the IMA 2012 naming system (Hawthorne et al. 2012).

Epidote is aligned in roughly parallel prisms. Crystals are pleochroic in thin section, appearing at different stages to be colorless, pale green, or pale yellow (Fig. 3). Crystals are around 2-3 mm in length and 1 mm in width and contain small inclusions of rutile and sphene as well as smaller glaucophane crystals (Fig. 5). Foliation is also evident in the alignment of epidote crystals at a 45° angle from the foliation of the amphibole, appearing to predate the amphibole foliation.

Garnets range in size, averaging around 3-4 mm in diameter. Garnets occur through the sample, but are concentrated in the vein (Fig. 2). Where several garnets are in close proximity, such as at the garnet vein, there are often crystals of colorless quartz between the garnet crystals (Fig. 5). Zoning is not evident in PPL, where garnets are reddish pink in coloration and ringed with dark chlorite (Fig. 3). Garnets are primarily zoned in manganese and iron, and have a core composition of $Alm_{56}Grs_{27}Pyp_{3}Sps_{14}$ and a rim composition of $Alm_{66}Grs_{25}Pyp_{9}Sps_{0}$ (Fig. 8).

Pyroxene forms long tabular crystals, in thin section these crystals are dark green and in high relief. Clinopyroxene is notably rich in ferric iron, with the composition $Ac_{13}Jd_{34}Di_{39}Hd_{11}CaTs_{1}$ (Fig. 9). Phengite is present as smaller crystals throughout the amphibole and surrounding the garnets, colorless in thin section with one direction of perfect cleavage (Fig. 3). Compositionally, the phengite lacks chemical zoning and has a composition of $KAl_{1.5}(Mg_{.36}Fe_{.21})(Al_{.5}Si_{3.5}O_{10})(OH)_{2}$.

Minerals evident in smaller quantities include sphene, rutile, quartz, and zircon. Rutiles are dark brown in thin section and are usually surrounded and intergrown with lightly colored sphene, indicating synchronous growth (Fig. 7). Quartz is found typically near to or between garnets, and is most evident around the garnet vein that propagates

through the sample (Figs. 2, 5). Quartz is completely recrystallized, with 60-120 grain boundaries indicating equilibrium textures. These textures obscure any strain path information that could be drawn from the quartz growth.

Because the blueschist clast is from a sedimentary breccia deposit, there is no reference frame for the foliation of the sample. Foliation is noticeable in elongation of the garnet with parallel amphibole grains, and in recrystallized quartz fabrics between garnets (Fig.5).

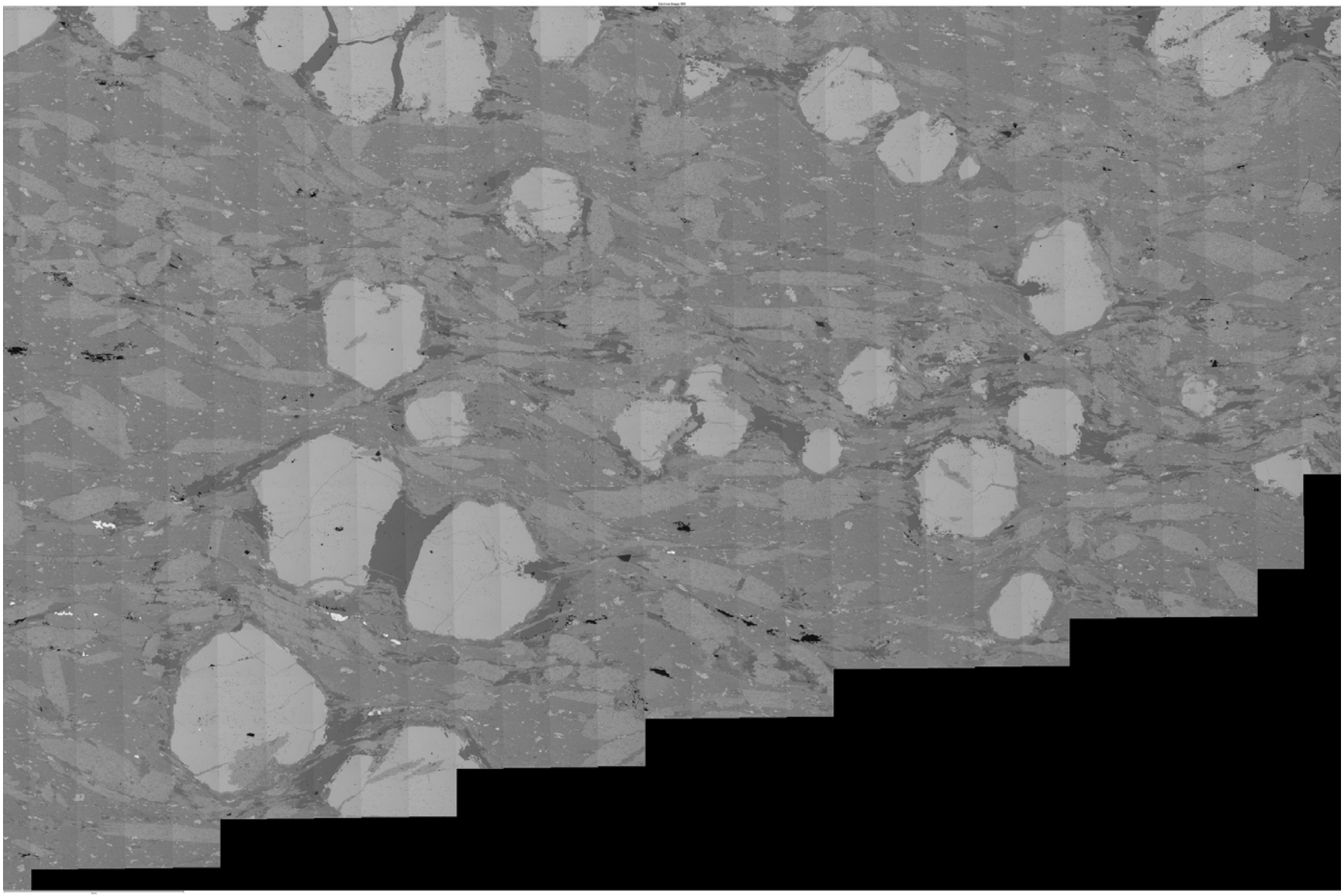

Figure 4. BSE image of the thin section used in bulk composition analysis

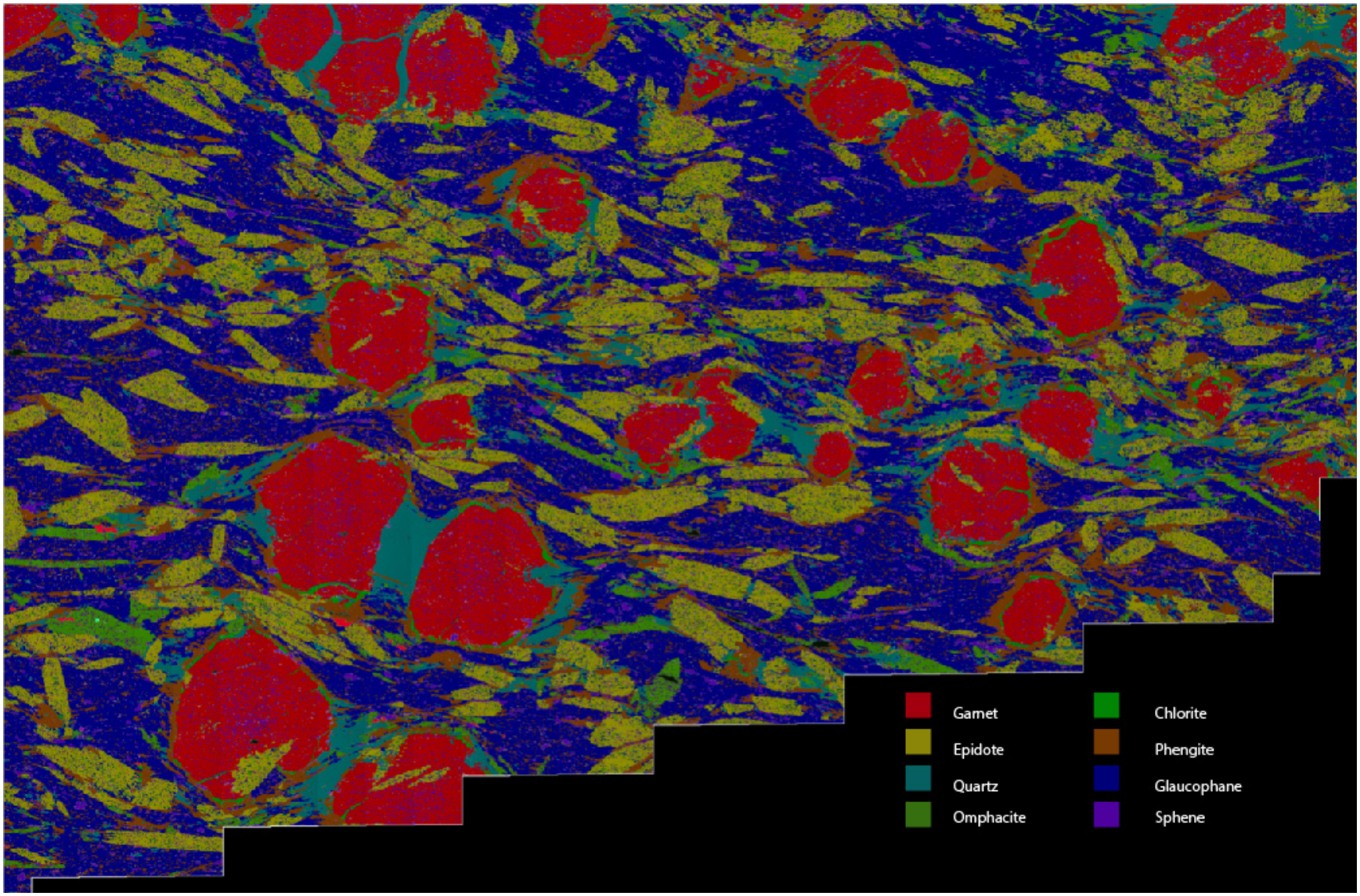

Figure 5. EDS phase maps of a thin section from the San Onofre Blueschist used for bulk composition analysis.Note the quartz only exists around garnets.

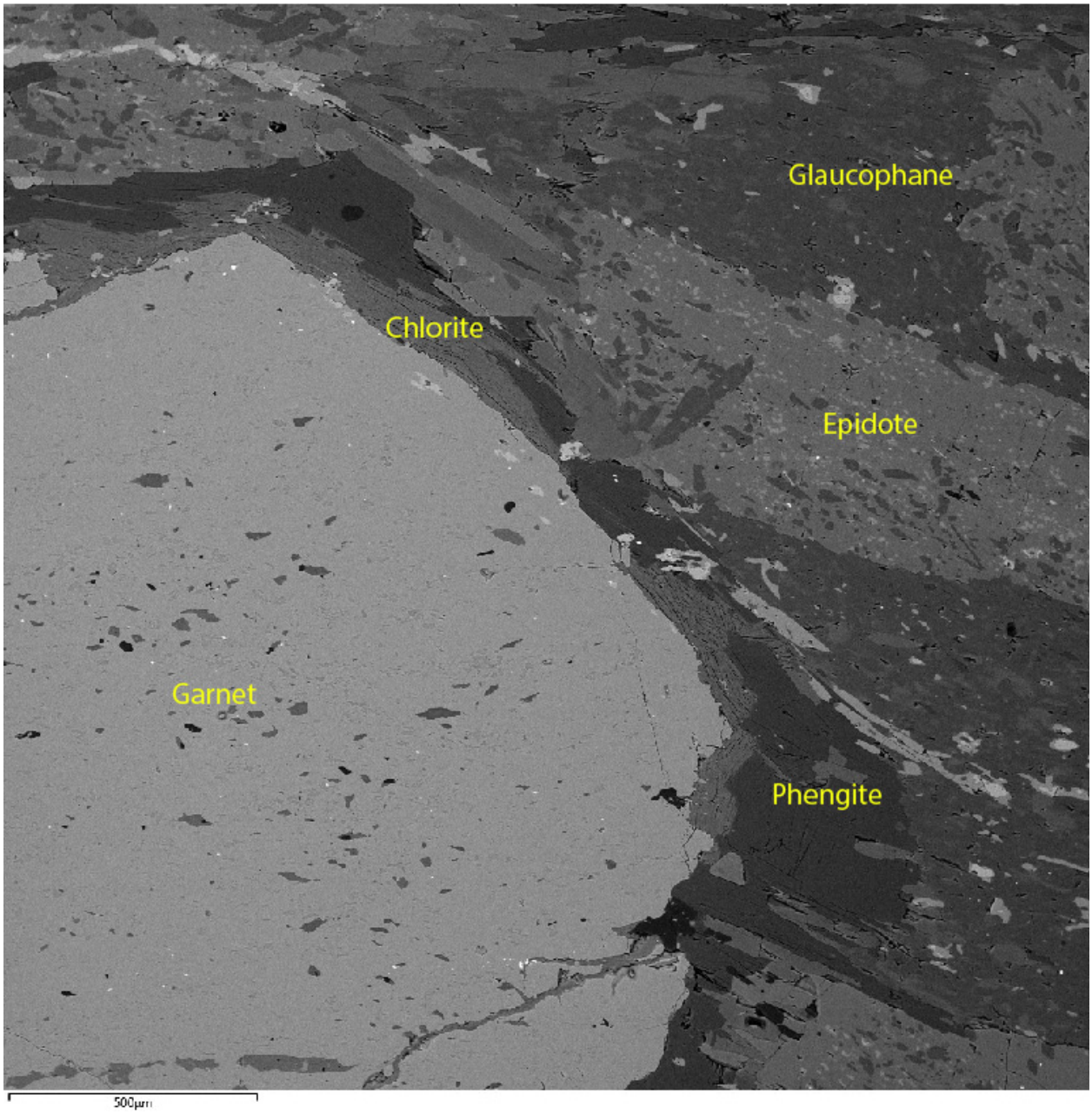

Figure 6. BSE image with epidote in upper right-hand corner.

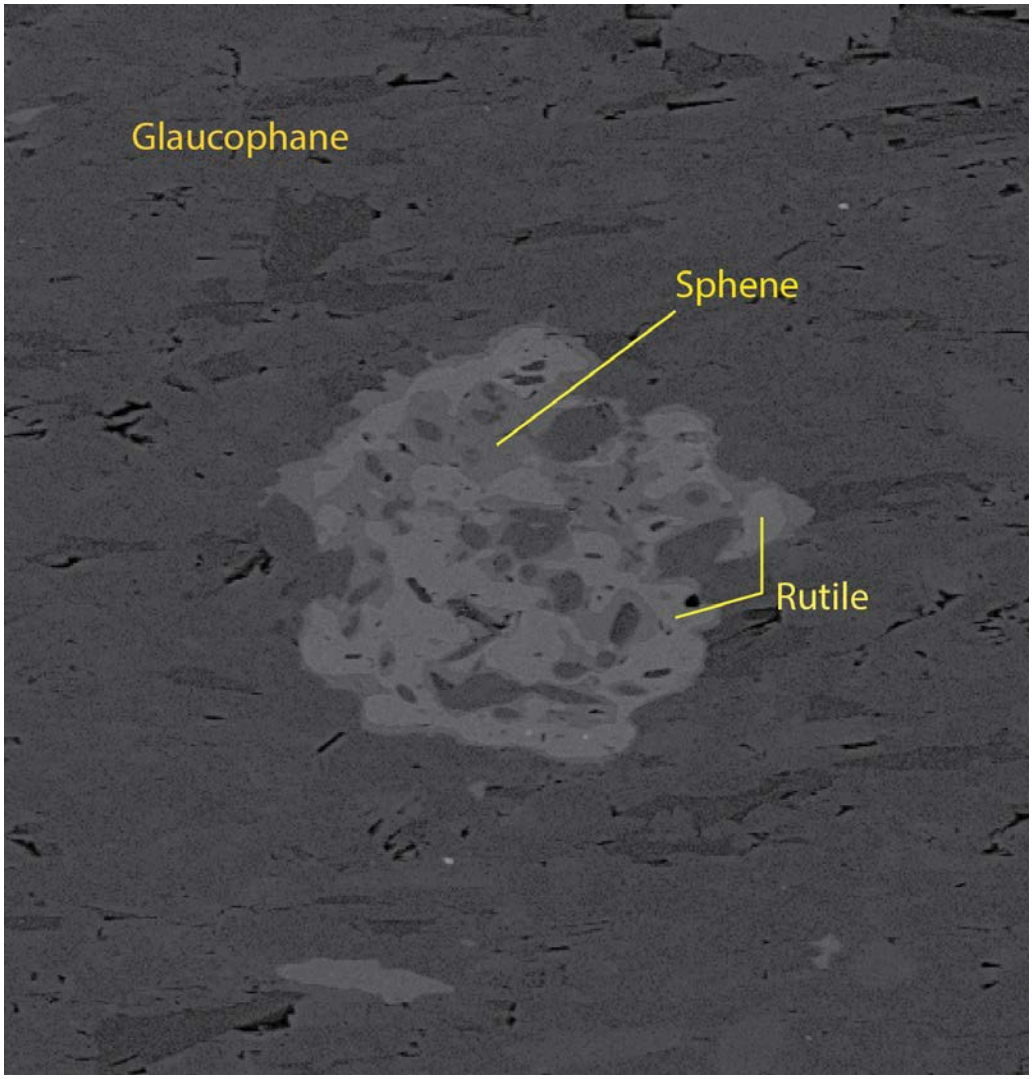

Figure 7. BSE image of an intergrown rutile and sphene crystal within the amphibole matrix. Sphene is darker than rutile.

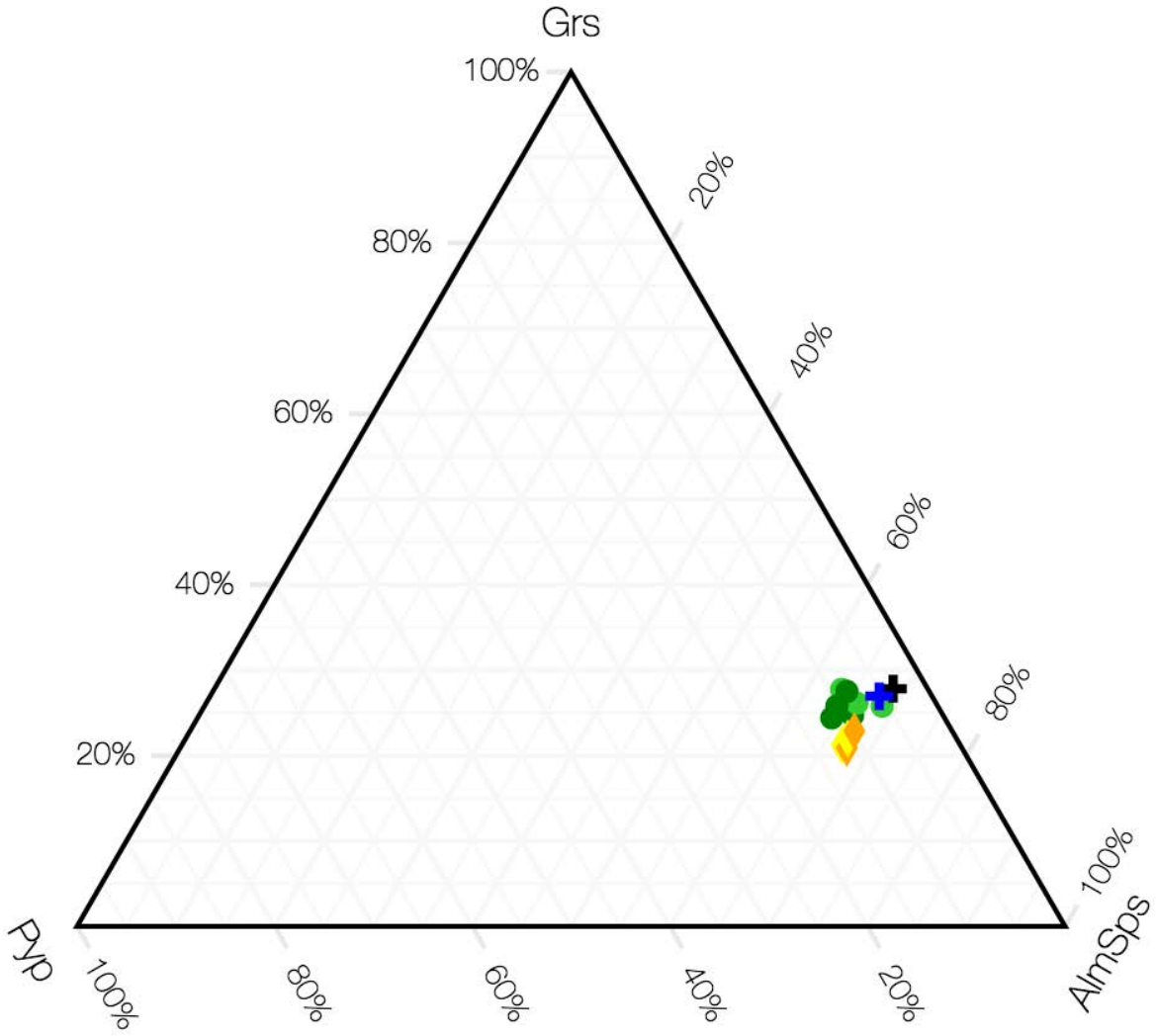

Figure 8. Garnet compositions in the San Onofre Blueschist. Green circles represent samples from San Onofre, Blue crosses are Franciscan garnets from Krogh et al. 1994, orange diamonds represent Catalina garnets from Adler-Ivanbrook et al. 2018. The lighter shade of each color represents core composition, and the darker shade represents rim composition.

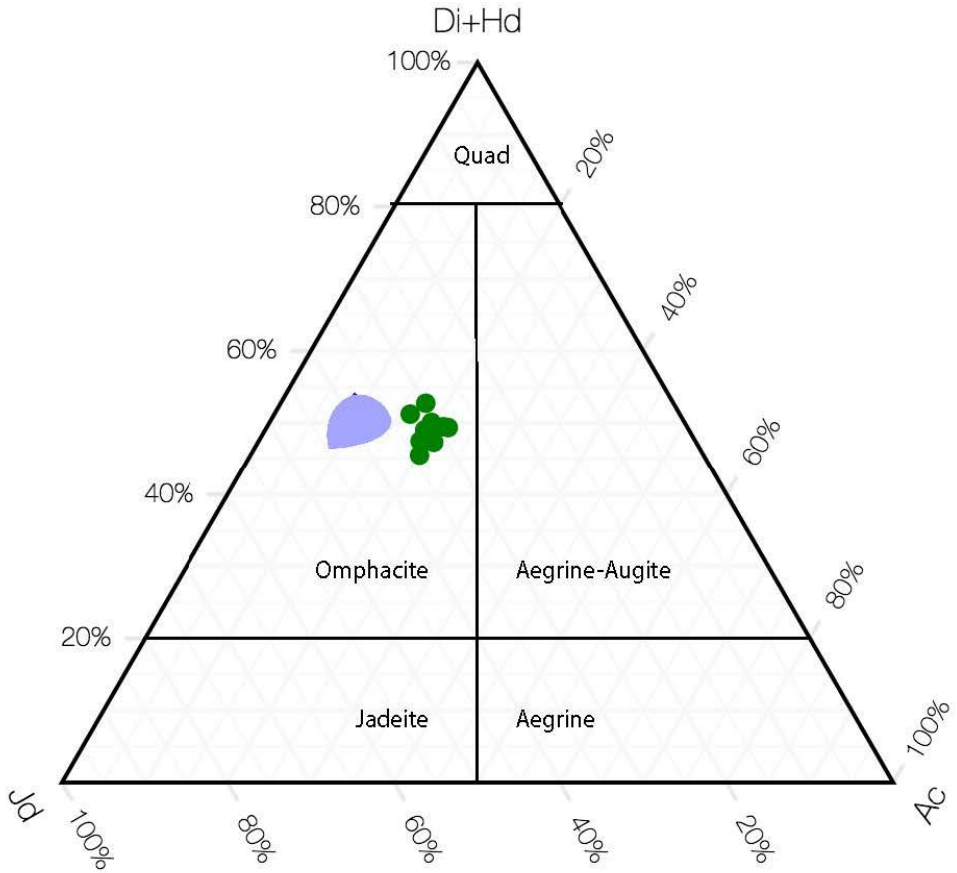

Figure 9. Pyroxene compositions. Green circles are from the San Onofre Breccia and the blue line shows the range of Franciscan omphacite compositions reported in Tsujimori et al. (2006).

Wt. %	San Onofre	MORB(Honshu)	AOC(Honshu)	Franciscan	Catalina
SiO_2	51.11	48.669	47.559	51.19	50.11
Na_2O	2.82	2.606	1.964	2.46	3.94
MgO	5.20	7.639	8.288	8.19	5.16
Al_2O_3	15.06	15.184	14.923	12.43	14.55
K_2O	1.46			2.61	1.63
CaO	9.38	10.954	12.132	6.18	5.1
TiO_2	3.18			1.42	17.66
MnO	0.19			0.66	0.602
FeO	11.56	9.122	8.749	13.69	13.84
P_2O_5	0.06			0.26	0.178

Table 1. Bulk composition of the San Onofre Blueschist sample 18SO-01 in comparison with Mid Ocean Ridge Basalt (MORB), Altered Oceanic Crust (AOC), and garnet blueschist samples from the Franciscan and Catalina. MORB and AOC compositions come from Walters et al. 2020, the Catalina composition comes from Awalt 2013 and the Franciscan composition is from Krogh et al. 1994.

Thermobarometry

Pressure-temperature estimates were completed using assemblage modeling techniques in Perple_X. The use of equilibrium assemblage diagrams to calculate the pressure and temperature of formation for the blueschist cobble predicts when the assemblage observed in a specific sample is chemically stable using Gibbs free energy. Bulk composition used in equilibrium assemblage modeling was from a section of the sample away from the garnet vein, assuming that the area surveyed is representative of the blueschist assemblage as a whole.

To replicate the assemblage observed in the sample from San Onofre, oxygen was added to the bulk composition of the assemblage to allow for the formation of ferric iron which is observed in epidote, pyroxene, and phengite. T-X and P-X diagrams were

used to estimate the amount of oxygen present in the system to reproduce the observed ferric-iron rich assemblages, as described in the methods section. Using this technique, we determined that less oxygen prevented the formation of epidote while too much oxygen caused the formation of minerals not observed in the assemblage such as ilmenite and magnetite. Using a variety of different pressure conditions, it was determined that the addition of about 0.3 wt% oxygen allowed assemblages matching the ones observed in the sample to be stable within the parameters of the model. Although the observed assemblage is predicted to be stable between 0.1 and 0.6 wt% oxygen, reducing the oxygen quantity caused there to be a smaller quantity of stable epidote within the model while increasing oxygen increased the amount of stable epidote and significantly reduced the amount of stable garnet. An example of one such T-X diagram used to constrain the necessary quantity of oxygen to be added to the system is Figure 10.

An equilibrium assemblage diagram created using the estimated value of 0.3 wt% oxygen was used to constrain pressure and temperature. The stability field of the observed assemblage on the equilibrium assemblage diagram is from 15 to 18 kbar and between 490 and 530 °C (Fig. 11). At higher pressures, there is no sphene predicted by the model, while lower pressures lack predicted rutile. The coexistence of rutile and sphene within the assemblage model is important because within the sample both rutile and sphene are intergrown, indicating that they formed synchronously. At lower temperatures, the model predicts the formation of lawsonite instead of epidote while increasing pressure causes actinolite to form in addition to glaucophane.

Modelled compositional isomodes of garnet, amphibole, and epidote were used to constrain the stability field of the assemblage based on where the observed mode of each mineral overlaps. The model predicts two different amphiboles depending on compositions, a more sodic glaucophane and a more calcic actinolite. Isomodes show a decrease in glaucophane as pressure and temperature increase, with some pressure-temperature ranges complicated by the formation of both types of amphibole within the model (Fig. 12). Epidote volume decreases as pressure and temperature rise, and epidote does not form at higher pressures with lower temperatures (Fig. 12). Garnet volume continuously increases as pressure and temperature increase (Fig. 12). The intersection of these isomodes indicates that the assemblage formed at 16 kbar of pressure at a temperature of around 520 °C when 0.3 wt% oxygen is included in the model. At these conditions, the predicted volume of all minerals observed in the model closely matches the observed assemblage. The model does not perfectly match the composition of each mineral, and underpredicts ferric iron. Within the model garnet is predicted to be a higher percent grossular, and lower in pyrope and spessartine ($Alm_{51}Grs_{40}Pyp_{0}Sps_{2}$). The projected pyroxene contains less acmite, diopside, and jadeite than is observed in the sample.

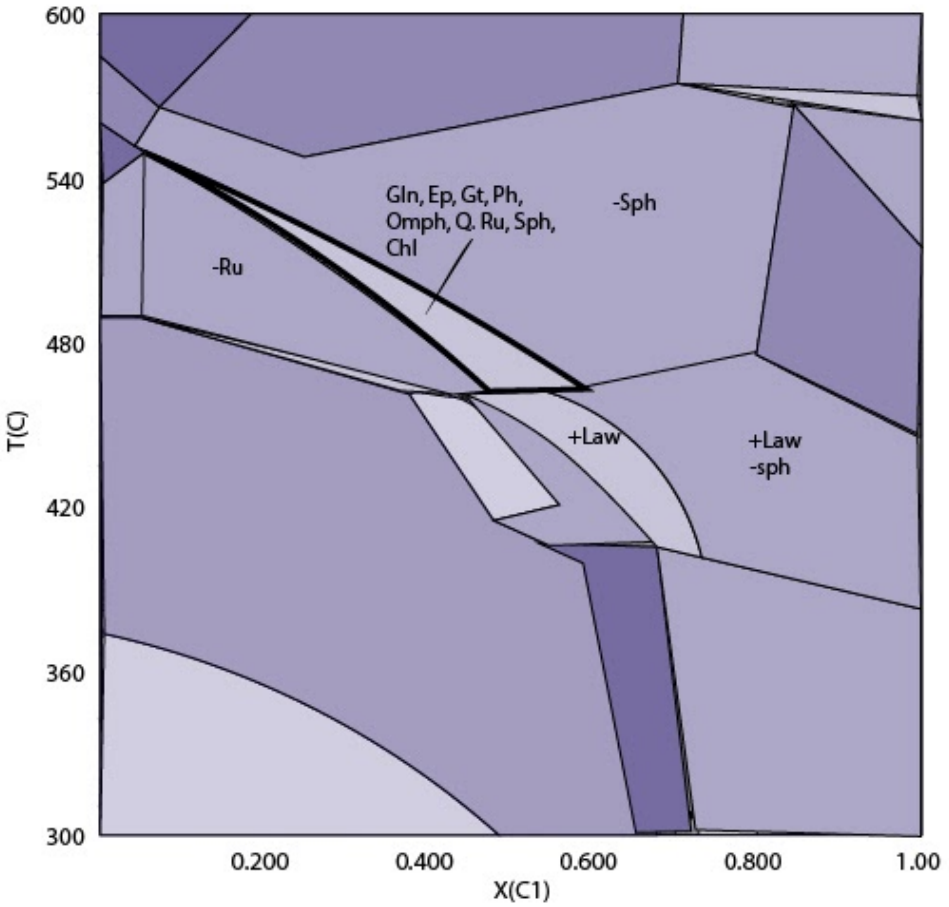

Figure 10. An example of a T-X diagram used to constrain the amount of oxygen required to allow the observed assemblage to be stable. Pressure is fixed at 16 kbar.

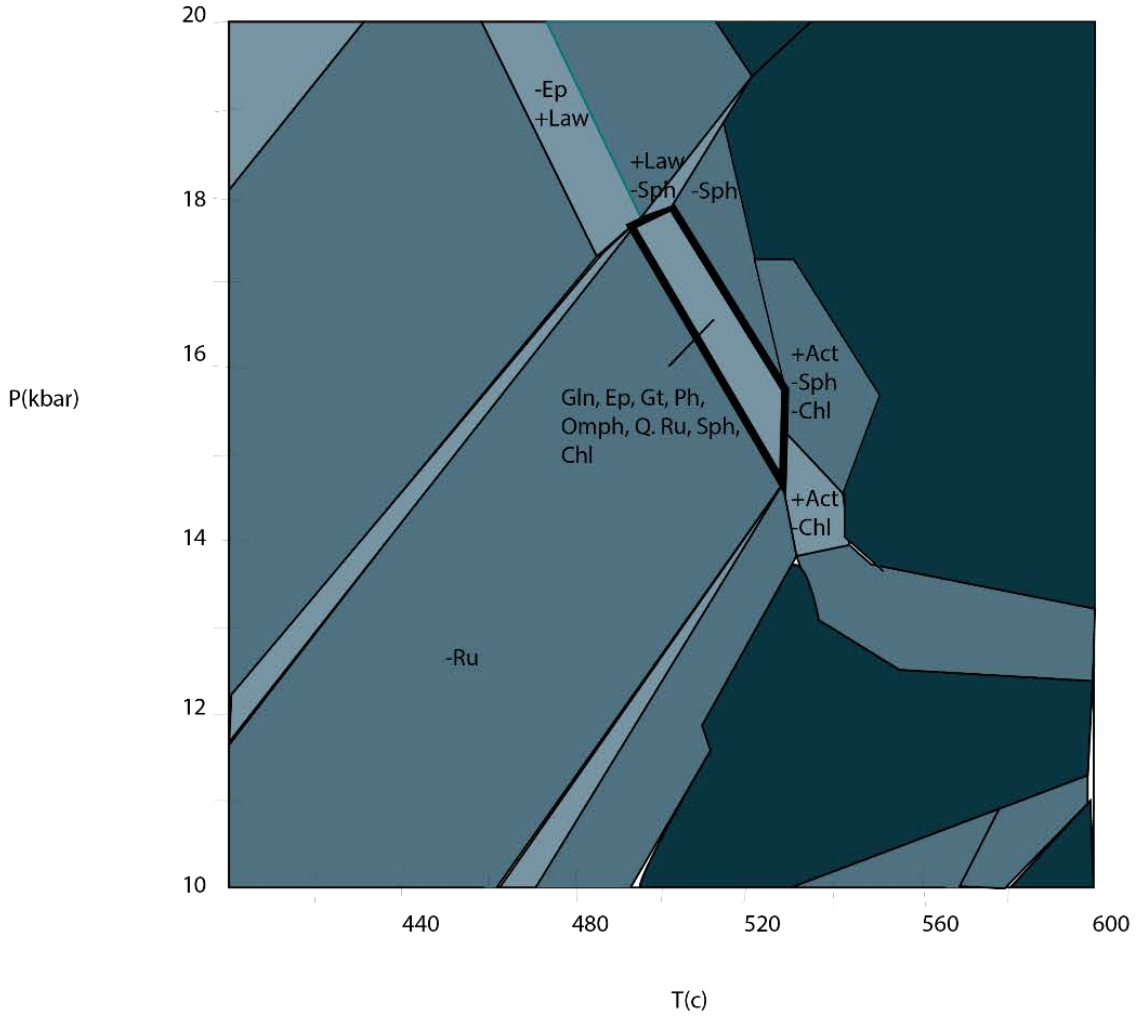

Figure 11. Equilibrium assemblage diagram. The predicted pressure-temperature field is within the bolded outline.

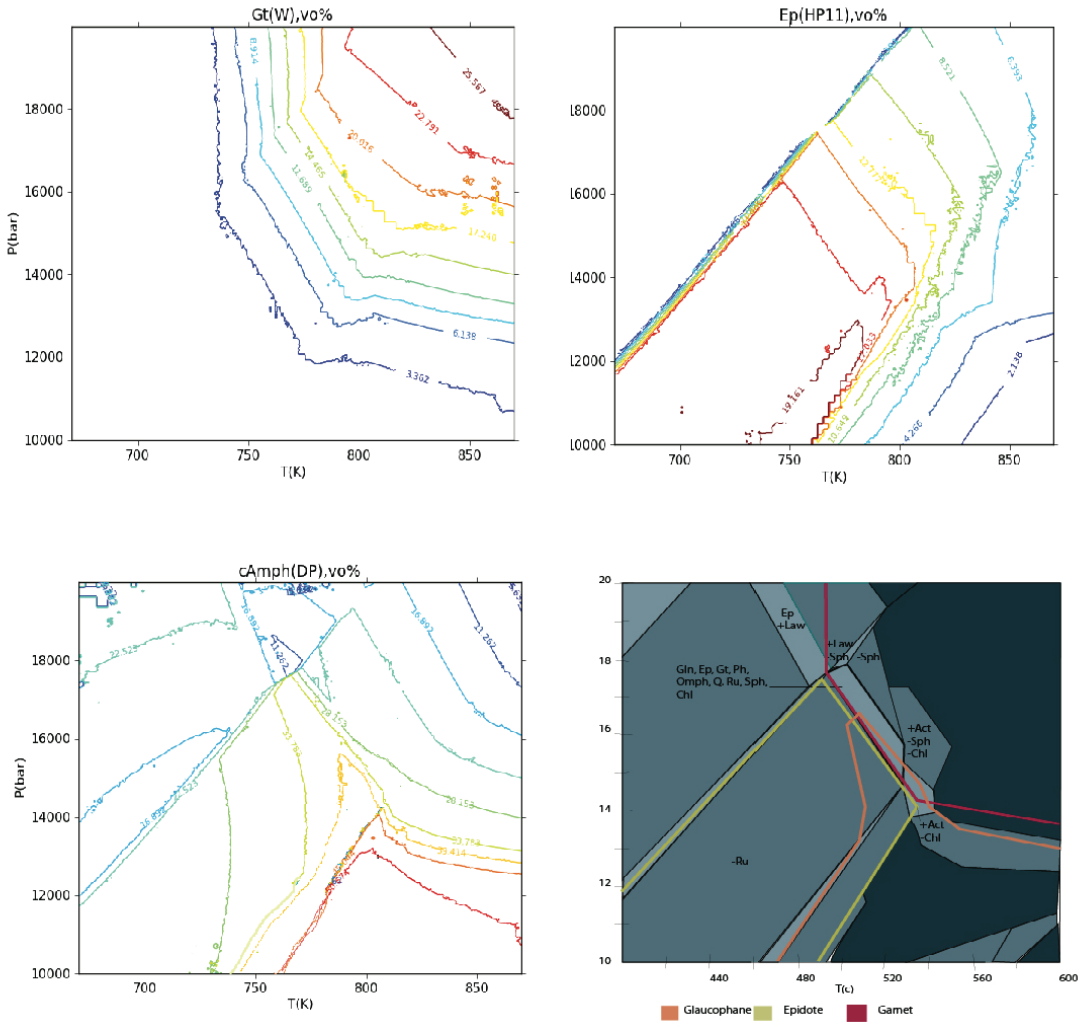

Figure 12. Mineral isomode diagrams of garnet, epidote, and amphibole. These graphs provide topographic lines mapping out the volume of each specific mineral phase at different temperature and pressure conditions. By overlaying mineral modes with the equilibrium assemblage diagram as shown in the bottom right, they can be used to help constrain pressure and temperature information about a specific assemblage. Where observed modes intersect, there is potential for the formation of the observed assemblage to be stable.

Discussion

Thermobarometry, geochemical, and mineralogical evaluations of the San Onofre Blueschist allow for the quantitative analysis of how the San Onofre Breccia's formation fits into the Franciscan and Catalina subduction cycles. Comparing the sample from San Onofre to other analyses from Catalina and Franciscan outcrops as well as with altered oceanic crust allows us to contextualize the samples' tectonic setting, and pressure-temperature information allows us to distinguish between the hotter and younger Catalina subduction and the cooler and older Franciscan subduction as the source of the blueschist.

Geochemical data comparing San Onofre Blueschist with Franciscan and Catalina blueschist bulk compositions as well as AOC and MORB are reported in Table 1. San Onofre bulk compositions were completed using a whole X-ray map as described in the methods as opposed to using an XRF sample. Using the EDS map to calculate the bulk composition ensures that the composition is representative of the whole thin section as opposed to specific points. AOC and MORB values are from Walters et al. 2020, the Franciscan Blueschist composition is from Krogh et al.1994, and the Catalina blueschist composition is from Awalt 2013. Sodium content is similar to that observed in the Franciscan and MORB datasets. Magnesium content from the San Onofre is very close to the magnesium content observed in the Catalina sample. Calcium content is greater than that observed in the Franciscan and Catalina blueschist samples, but less than MORB or AOC. Geochemical analysis of a cobble of garnet-epidote blueschist from San Onofre shows some variation from Catalina Schist as the

San Onofre sample is oxidized and richer in calcium than samples from Catalina, possibly indicating a different source.

When compared mineralogically, Catalina island amphiboles are less calcium rich than the San Onofre sample and epidotes are less common (Walters et al. 2020, Awalt 2013). Pyroxenes within the San Onofre Blueschist are omphacitic, similar in composition to those observed by Krogh et al.1994 in Franciscan Blueschists (Fig. 9). The San Onofre Blueschist's amphibole is similar to amphiboles found in Franciscan schist assemblages described in Krogh et al. 1994 which found at different stages of metamorphism blueschist contained barroisite and winchite. Awalt found Catalina's blueschist to be more commonly glaucophane and winchite in terms of composition (Awalt 2013). Additionally, the San Onofre blueschist exhibits high amounts of ferric iron in epidote and phengite.

Assemblage modeling of Franciscan and Catalina schist samples provides some context to the origin of the clasts in the San Onofre Breccia. Equilibrium assemblage modeling allows for the pressure and temperature to be estimated within the constraints of both mineral stability and mineral composition within a specific rock. Franciscan and Catalina assemblages both include blueschist, which tend to form at higher temperatures in the Catalina than in the Franciscan. Additionally, lawsonite tends to form instead of epidote under higher pressure conditions. Harvey et al. 2020 reports temperature and pressure conditions of formation for a Catalina garnet blueschist facies block at 635 $\pm$ 14 °C at 16.5 kbar of pressure using Zr-in-rutile thermometry and Quartz-in-garnet barometry (Fig. 14). Krogh et al. 1994 reports Franciscan retrograde blueschist to have predicted P–T conditions at around 480° C at 14 kbar calculated

using thermocalc(Fig. 14). Similar Franciscan blueschist samples have also been described more recently by Tsujimori et al. (2006), which have minimum retrograde conditions at 7 to 8 kbar and 350° C. Tsujimori does not describe pressure-temperature conditions at peak metamorphism.

Rocks found on Catalina are typically quartzites and amphibolites (Grove et al. 2008). Blueschists on Catalina are more commonly lawsonite blueschists (Grove et al. 2008). Epidote blueschists found on Catalina do not have garnets (Grove et al. 2008). Additionally, Grove et al. suggests that epidote blueschists likely formed in a separate Franciscan subduction zone than lawsonite blueschists on Catalina. The pressure-temperature estimates for lawsonite blueschist and amphibolite mélange show a hotter pressure-temperature path than that observed in the blueschist from San Onofre, existing on a different geothermal gradient (Fig. 14). Krogh et al's estimated pressure and temperature conditions for a retrograde garnet-bearing epidote blueschist falls on the same geothermal gradient as the blueschist from the San Onofre Breccia when comparing thermodynamic modeling results in Figure 14. The differing characteristics between Catalina and Franciscan blueschists leads one to conclude that garnet-bearing epidote-blueschists are more similar to the San Onofre Blueschist.

One major challenge which impacts our modeling results is the inclusion of oxygen within the model to allow for ferric iron necessary to form the oxidized mineral assemblage observed in the sample from San Onofre. Estimates for the amount of oxygen to include in the model were based of P-X and T-X modeling to find where assemblages closest matching our observed assemblage were predicted to be stable. This technique is limited to the accuracies of the thermocalc database used by

Perple_X, for which uncertainties are difficult to quantify. Uncertainties may be slightly higher because of the Fe^{3+}, but the San Onofre Blueschist is so different from the Catalina Blueschist that such errors are unlikely to change the results. In addition to the challenges of modeling such a highly oxidized system, it is also important to consider how limitations to the chemical system used in the model could over-simplify a complex natural system (Spear et al. 2016). Similarly oxidized samples from Sifnos in Greece have been analyzed using the N(K)CFMASHO system (Gruppo et al. 2008), which provides precedence for the modeling of an oxidized garnet-epidote blueschist with the addition of oxygen to allow for Fe^{3+} formation.

Highly oxidized rocks such as this example from the San Onofre Breccia would have been influenced by the presence of concentration and speciation of elements responsive to redox reactions. In Walters et al. 2020 it is proposed that the presence of sulfur in slab derived subduction can result in the oxidation of the mantle wedge. The composition of 18So1b is stable with the inclusion of about 0.3 wt% oxygen, similar to the models of Altered Oceanic Crust (AOC) from Walters et al. 2020 but lacks sulfur.

Calculation of the amount of oxygen, and ferric iron in the blueschist presents many areas of potential error. Calculation of Fe^{3+} is often subject to analytical error and uncertainty, and without access to Mossbauer spectroscopy as an analytical method that would more precisely determine the ratio of Fe^{3+}/Fe^{2+} results of conventional garnet pyroxene thermobarometry can be inconsistent (Proyer et al. 2004). Perple_X modeling is also not without it's shortcomings as equilibrium models consistently over-predict the amount of Fe^{3+} in Amphiboles while under-predicting Fe^{3+} in omphacite. Such inconsistencies are less significant when using multi equilibrium techniques (Proyer et al. 2004), making assemblage modeling with Perple_X less problematic. Petrological analysis

suggests that the San Onofre Blueschist is different from blueschist samples associated with the Catalina subduction cycle, and may be from a different subducting trench and more closely related to Franciscan subduction. It is probable that more Franciscan-aged material existed offshore during the Eocene, and to more definitively determine the relationship between the metamorphosed cobbles from the San Onofre Breccia and the Catalina subduction zone more clasts should be sampled and dated.

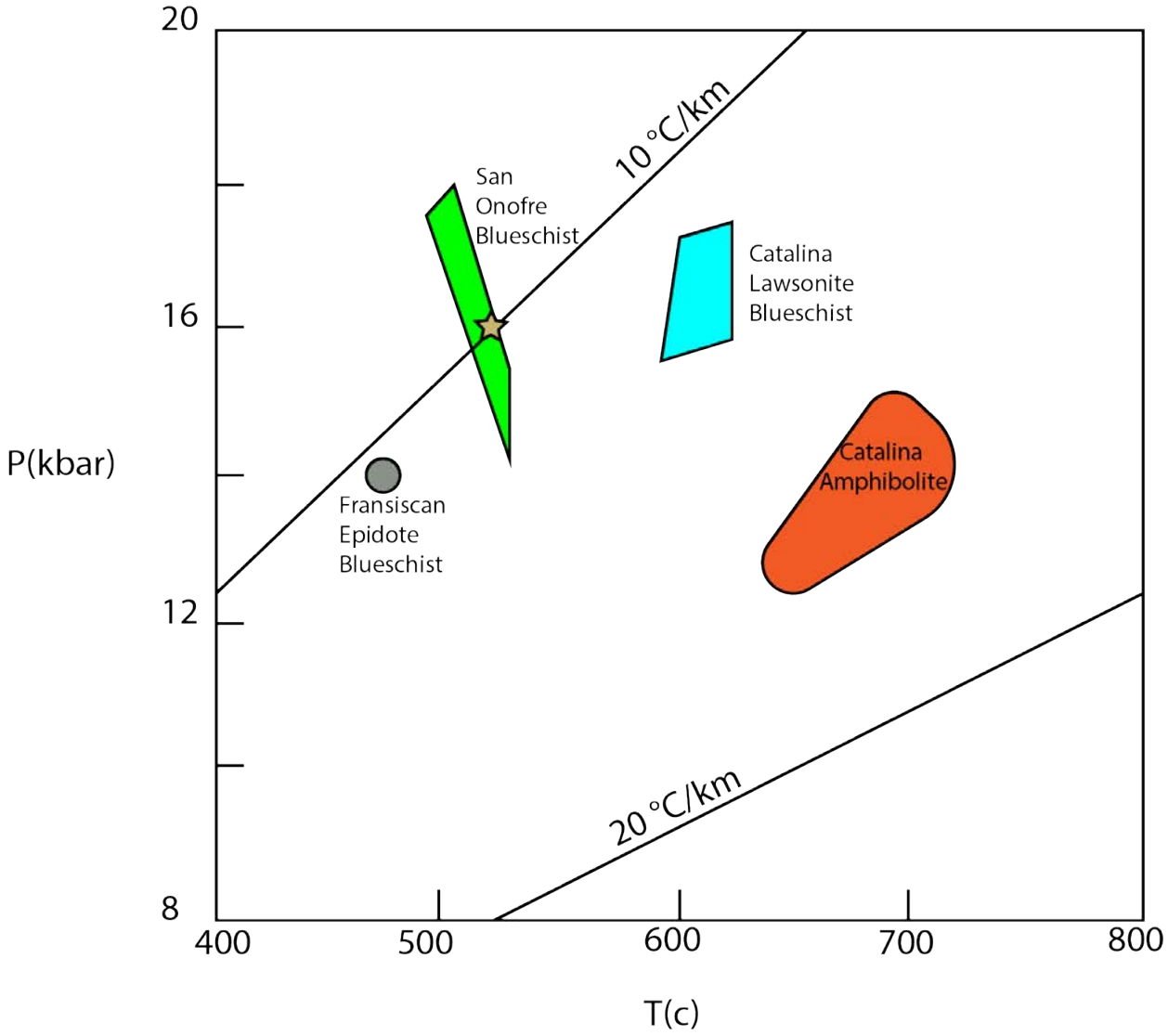

Figure 13. Pressure temperature fields from Catalina, the Franciscan, and San Onofre in relation to geotherms. Geotherms are from Penniston-Dorland et al. 2015. The green field represents the stability range of the assemblage observed in the San Onofre Blueschist. The yellow star represents the point of the specific assemblage from San Onofre. The grey point shows the predicted pressure and temperature of Franciscan garnet bearing epidote blueschist from Krogh et al. 1994. In blue is Catalina lawsonite blueschist and red is Catalina amphibolite from Harvey et al. 2020.

Acknowledgements

I would like to especially acknowledge Dr. Jade Star Lackey for research assistance and providing the blueschist specimen, Dr. Steve Wojtal for his assistance completing thin section analysis, Josie Boyd for assistance in sample preparation. Lastly, many thanks to Dr. F. Zeb Page for his continuous support and assistance throughout the research process.

References

Adler-Ivanbrook B, Hampton SK, Esparza Limon JP, Lackey JS, and Page FZ (2018) An investigation of the Catalina garnet-blueschist: Major and trace element composition and zoning in garnet and lawsonite from a multiply subducted block, Abstract T21F-0290 presented at 2018 AGU Fall Meeting, Washington, DC 10-14 Dec.

Awalt, M.B., 2013, Petrology and Pseudosection Modeling of a Garnet-Blueschist Block-in-Melange, Santa Catalina Island, CA [thesis].

Connolly, J.A.D. (1990) Multivariable phase diagrams: an algorithm based on generalized thermodynamics. American Journal of Science, 290, 666–718.

Connolly, J.A.D. (2005) Computation of phase equilibria by linear programming: A tool for geodynamic modeling and its application to subduction zone decarbonation. Earth and Planetary Science Letters, 236, 524–541

Crouch, J.K., and Suppe, J., 1993, Late Cenozoic tectonic evolution of the Los Angeles Basin and inner California borderland; a model for core complex-like crustal extension: Geological Society of America Bulletin, v.105, p.1415-1434,

Diener JFA, Powell R, White RW,Holland TJB (2007) *A new thermodynamic model for clino- and orthoamphiboles in the system Na2O-CaO-FeO-MgO-Al2O3-SiO2-H2O-O*. Journal of Metamorphic Geology **25**:631-56.

Fuhrman ML,Lindsley DH (1988) *Ternary-Feldspar Modeling and Thermometry*. American Mineralogist **73**:201-15.

Green E, Holland T,Powell R (2007) *An order-disorder model for omphacitic pyroxenes in the system jadeite-diopside-hedenbergite-acmite, with applications to eclogitic rocks*. American Mineralogist **92**:1181-9.

Groppo, C., Forster, M., Lister, G., and Compagnoni, R., 2009, Glaucophane schists and associated rocks from Sifnos (Cyclades, Greece): New constraints on the P–T evolution from oxidized systems: Lithos, v. 109, p. 254–273.

Grove, M., Bebout, G., Jacobson, C., Barth, A., Kimbrough, D., King, R., Zou, H., Lovera, O., Mahoney, B., and Gehrels, G., 2008, The Catalina Schist: Evidence for middle Cretaceous subduction erosion of southwestern North America: Special Paper 436: Formation and Applications of the Sedimentary Record in Arc Collision Zones, p. 335–361.

Harvey, K.M., Penniston-Dorland, S.C., Kohn, M.J., and Piccoli, P.M., 2020, Assessing P-T variability in mélange blocks from the Catalina Schist: Is there differential movement

at the subduction interface?: Journal of Metamorphic Geology, v. 39, p. 271–295, doi: 10.1111/jmg.12571.

Hawthorne, Frank & Oberti, Roberta & Harlow, George & Maresch, Walter & Martin, R.F. & Schumacher, John & Welch, Mark. (2012). IMA report: Nomenclature of the amphibole supergroup. American Mineralogist. 97. 2031-2048. 10.2138/am.2012.4276.

Holland, T.J.B. & Powell, R., 2003. Activity-composition relations for phases in petrological calculations: an asymmetric multicomponent formulation. Contributions to Mineralogy and Petrology, 145, 492–501.

Holland, T.J.B. & Powell, R., 2011. An improved and extended internally consistent thermodynamic dataset for phases of petrological interest, involving a new equation of state for solids. Journal of Metamorphic Geology, 29, 333–383.

Krogh, E. J., Oh, C. W. & Liou, J. G., 1994. Polyphase and anticlockwise P–T evolution for Franciscan eclogites and blueschists from Jenner, California, USA. Journal of Metamorphic Geology, 12, 121–134.

Locock, A.J., 2014, An Excel spreadsheet to classify chemical analyses of amphiboles following the IMA 2012 recommendations: Computers & Geosciences, v. 62, p. 1–11, doi: 10.1016/j.cageo.2013.09.011.

Penniston-Dorland, S.C., Kohn, M.J., and Manning, C.E., 2015, The global range of subduction zone thermal structures from exhumed blueschists and eclogites: Rocks are hotter than models: Earth and Planetary Science Letters, v. 428, p. 243–254.

Proyer, A., Dachs, E. & McCammon, C. (2004). Pitfalls in geothermobarometry of eclogites: Fe3þ and changes in the mineral chemistry of omphacite at ultrahigh pressures. Contributions to Mineralogy and Petrology 147, 305-318.

Platt*, J.P., Grove*, M., Kimbrough*, D.L., and Jacobson*, C.E., 2020, Structure, metamorphism, and geodynamic significance of the Catalina Schist terrane: From the Islands to the Mountains: A 2020 View of Geologic Excursions in Southern California, p. 165–195, doi: 10.1130/2020.0059(05).

Platt, J.P., 1975, Metamorphic and deformational processes in the Franciscan Complex, California: Some insights from the Catalina Schist terrane: Geological Society of America Bulletin, v. 86, p. 1337–1347

Krogh Ravna E, Terry MP (2004) Geothermobarometry of UHP and HP eclogites and schists – an evaluation of equilibria among garnet-clinopyroxene-kyanite-phengite-coesite=quartz. J Metamorph Geol 22: 579–592

Sorensen, S. 1972 Petrology of San Onofre Breccia “Megaclasts”, San Onofre Mountain, California.

Spear, Frank S., Pattison, David R.M., Cheney,John T. , 2017, The Metamorphosis of Metamorphic Petrology, The Web of Geological Sciences: Advances, Impacts, and Interactions II, Marion E. Bickford

Stuart, C.J., 1974, The San Onofre Breccia in Northwestern Baja California and Its Regional Tectonic Implications, *in* The Geology of Peninsular California, 49th Annual Meeting, p. 80–90.

Stuart, C.J., 1979, *in* A guidebook to Miocene lithofacies and depositional environments, coastal Southern California and northwestern Baja California, Los Angeles, Pacific Section, Society of Economic Paleontologists and Mineralogists, p. 25–42.

Sun, S.S. & McDonough, W.F., 1989, Chemical and isotopic systematics of oceanic basalts: implications for mantle compositions and processes. In: Magmatism in the Ocean Basins, Special Publications of the Geological Society of London (eds Saunders, A. & Norry, M.), v. 42, p. 313–345.

Tsujimori, T., Matsumoto, K., Wakabayashi, J., and Liou, J.G., 2006, Franciscan eclogite revisited: Reevaluation of the P–T evolution of tectonic blocks from Tiburon Peninsula, California, U.S.A.: Mineralogy and Petrology, v. 88, p. 243–267.

Vedder, J. G. and Howell J. G., 1976, Distribution and Tectonic Implications of Miocene Debris From the Catalina Schist, California Continental Borderland and Adjacent Coastal Areas: AAPG Datapages/Archives.

Wakabayashi, J., 1999, Subduction and the rock record: Concepts developed in the Franciscan Complex, California: Classic Cordilleran Concepts: A View from California, doi: 10.1130/0-8137-2338-8.123.

White, R.W., Powell, R., Holland, T.J.B., Johnson, T.E. & Green, E.C.R., 2014. Progress relating to calculation of partial melting equilibria for metapelites. Journal of Metamorphic Geology, 25, 511–527.

Walters, J.B., Cruz-Uribe, A.M., and Marschall, H.R., 2020, Sulfur loss from subducted altered oceanic crust and implications for mantle oxidation: Geochemical Perspectives Letters, p. 36–41, doi: 10.7185/geochemlet.2011.

Wright, T.L., 1991, Structural geology and tectonic evolution of the Los Angeles Basin, California, in Biddle, K.T., ed., Active Margin Basins: American Association of Petroleum Geologists Memoir 52, p. 35-134.

Woodford, A.O., 1924 The Catalina metamorphic facies of the Franciscan Series: University of California Department of Geological Sciences Bulletin, v. 15, no. 3, p. 49-68.

Woodford, A. O., 1925, The San Onofre Brec- cia; its nature and origin: California Univ. Pubs. Geol. Sci., v. 15, p. 159-280.

Yeats, R.S., 1970, Stratigraphic Evidence for Catalina Schist Basement North of Channel Islands, California: Geological Society of America Bulletin, v. 81, p. 2147.